International Journal of Development Mathematics Vol 2 Issue 3 Page No. 001 - 023

INTERNATIONAL JOURNAL OF DEVELOPMENT MATHEMATICS

ISSN: 3026-8656 (Print) | 3026-8699 (Online)

journal homepage: https://ijdm.org.ng/index.php/Journals

Velocity Slip Effect on Unsteady Magnetohydrodynamic (MHD) Flow of Casson Fluid in the presence of Soret and Heat Source Mechanisms

Farisa Muhammad[a*], Emmanuel Omokhuale[a], Salisu M. Muhammad[a] and Lawal Sa'adu[b]

[a]Department of Mathematical Sciences, Federal University Gusau, P. M. B. 1001, Zamfara State, Nigeria.

[b]Department of Physics, Federal University Gusau, P. M. B. 1001, Zamfara State, Nigeria.

ARTICLE INFO

Article history:
Received 04 May 2025
Received in revised form 10 August 2025
Accepted 20 August 2025

Keywords:
Velocity slip; MHD; Casson fluid; Soret and Heat Source.

MSC 2020 Subject classification:
37N10

ABSTRACT

Velocity slip effect on unsteady Magnetohydrodynamic (MHD) flow of Casson fluid in the presence of Soret and heat source mechanisms has been studied. The governing equations are: momentum, energy and mass equations. The governing partial differential equations (PDEs) of the problem are transformed from dimensional to dimensionless forms using appropriate variables. The non-linear coupled PDEs are solved analytically by regular perturbation method to obtain the velocity, temperature and concentration of the fluid. The coefficients for skin-friction, Nusselt and Sherwood numbers were also derived. Computations were performed for important flow parameters viz. Thermal diffusion (Soret), heat source parameter, magnetic field parameter, Prandtl number, thermal radiation, thermal and mass Grashof number and Schmidt number which were graphically shown and discussed. The obtained results have been validated with published studies. The most significant conclusion of this work is that as Soret number and Casson parameter increase the velocity of the fluid becomes higher while a reverse trend is seen as heat source parameter is increased. Additionally, the mass boundary layer of the fluid rises due to an increase in Soret parameter while an opposite trend is observed in the temperature of the fluid because of increase in the heat source.

1. Introduction

The fluid is a specific type of matter which easily goes under deformation when an external force is applied, and it has no particular shape. Mainly, fluids are partitioned as Newtonian fluid and non-Newtonian fluids. Non-Newtonian fluids have numerous practical and industrial applications, and such fluids involve honey, blood, greases, oils, and food stuff (Anwar *et al.,* 2021). The boundary layer problems are given more consideration nowadays, this may not be unconnected with roles it plays in the areas of technology, engineering and industrial applications. Radiation effects on heat and mass transfer are of greater importance in many processes and have, therefore, received a considerable amount of attention in recent time, for example nuclear reactor, solid matrix heat exchanger, thermal insulation, surface catalysis of chemical contaminants in various processes, storage of nuclear waste materials, grain storage and drying and many others (Ahmad & Sarki, 2023). It is applied in engineering fields and physiology such as transpiration, cooling gaseous diffusion and blood flow in arteries. The flow through the porous media occurs on the

* Corresponding author. Tel.: +2348135521056
E-mail address: farisamuhammad02@gmail.com (Farisa Muhammad)
https://doi.org/10.62054/ijdm/0203.01

ground water hydrology. Irrigation and drainage problems are critical areas of greater concern, henceforth, scientific treatment of the problems of irrigation, soil erosion and tile drainage are some of the recent developments of porous media. Several researches indicated significant effects of slip condition on many problems of physical interest, among which are boundary layer flow control, plasma studies, geothermal energy extraction, metallurgy, chemical, mineral and petroleum engineering to mention but few (Ahmad & Sarki, 2023). The Casson type of fluids can be classified as non-Newtonian containing a yield stress which needs to be overcome followed by shear-thinning where viscosity is reduced as shear rate is increased. It was initially introduced to account for the flow of ink on the printing surface (Casson, 1959), which is now commonly used for modelling blood, chocolate, honey, polymers and other polymeric substances. Moreover, Casson fluids also have wide applications. Its importance among non-Newtonian fluids lies in its capability to mimic dual effects of yield stress and shear thinning which makes it applicable widely for biological and industrial processes where both effects are of utmost importance. For example, considering the blood's flow characteristics, the Casson model is applicable in hemodynamic since it applies to small vessels and explains the character of blood flow which is dependent on turbulence viscosity and yield stress. In engineering applications, Casson fluids provide an understanding of flow behavior characteristics of practice being a flow above a certain point is required and lock for processes involving more than one fluid the flow rate is of utmost importance. Due to their unique properties, Casson fluids are fundamentally important for modelling and optimizing numerous processes that require a greater degree of control over fluid dynamics. Casson fluid properties, which closely mimic blood flow in capillaries, are particularly relevant for designing biomedical devices like artificial organs. Additionally, studying heat and chemical reactions in fluid flows contributes to understanding pollutant dispersion from industrial sources and improving combustion efficiency to reduce emissions (Krishna & Reddy, 2025). In their study, numerical computations were performed to analyze the unsteady mixed flow of Casson fluid over an oscillatory slanted plate embedded in a permeable medium, under the influence of an angled magnetic field, heat source, thermal radiation, thermos diffusion, diffusion thermo, and chemical reactions.

Magnetohydrodynamics (MHD) is a discipline of physics that discusses the properties of an electrically conducting fluid when it is exposed to a magnetic field. Numerous industrial applications can be found for these MHD principles, such as flow meters, generators, and MHD Pumps. MHD principle is well-exemplified by dynamo and motor. Many researchers are interested in MHD topics such as geophysics, Astrophysics, and plasma physics among others, and also find in biology and medicine (Goud & Reddy, 2022). Chaudhary *et al.* (2025) investigated the magnetohydrodynamic boundary layer flow of Casson fluid

due to a moving permeable plate with Soret and Dufour impacts. Rajakumar *et al.* (2020) examined influence of radiation absorption and viscous dissipation on MHD free convective flow of Casson fluid model past a semi-infinite vertical porous plate. Multiple regular perturbation law was utilized for solving non dimensional governing equations.

Goud *et al.* (2023) discussed the impacts of velocity, temperature, and solutal slip on the mass and heat transfer characterization of MHD mixed convection Casson fluid flow along an exponential permeable stretching surface with chemical reaction, Dufour and Soret effects. The Casson fluid is supposed to flow across an exponentially stretched sheet, together with the exponential temperature and concentration fluctuations of the fluid. Akolade *et al.* (2021) investigated Soret–Dufour and multislip's impact on magnetohydrodynamics (MHD) Casson fluid flow encompassing variable thermophysical features in the nonlinear convection process is analyzed. It is believed that to any effective heat and mass transfer enhancement, the relaxation of such fluid and material time along with the thermo-physical features, are well estimated. In their model, a magnetic field of nonuniform strength is applied perpendicular to the slendering sheet with variable thickness, and nonlinear convection flow is considered in this generalized heat flux examination. Usman *et al.* (2022) discussed the impact of a chemical reaction and a magnetic field on unstable natural convection flow in a vertical porous channel. Babu *et al*. (2018) explained how the Soret and Dufour effects affect mass and heat transfer in chemically reacting MHD flow via a wavy channel. A study conducted by Uwanta and Hamza (2014) investigated the influence of the Soret and Dufour effects on the flow of free convective heat and mass transfer in a channel with constant suction and viscous dissipation. Then again, mass flux is able to be made by a temperature gradient as was recognized by Soret. This is the thermal-diffusion effect (Srinivas *et al.*, 2022). Furthermore, a phenomenon of thermo-diffusion in liquids was presented by Soret in 1879, and observed that concentration gradient is a happen cause of temperature gradient in a direct diffusion. In several applications, the effect of Soret is often neglected, since the order of magnitude is smaller than the effect described by Fourier's and Fick's laws. However, the effect become significant when the species having lower density than the surrounding liquids are introduced at surface of fluid medium. Also, such effect plays a vital role in the field of geosciences, oceanography, chemical engineering and air pollution (Ullah *et al.*, 2017). The Soret effect is a balance between thermal diffusion and mass diffusion (Jangid and Kolla, 2025).

Heat generation can be used in post-accident heat removal, fluids undergoing the exothermic process, and cooling of electronic components (Ahmad *et al.* 2023). Moreover, effects of heat generation/absorption on free convection MHD flow has considerable importance for many scientific and engineering applications.

On the other hand, flow in porous media has practical applications in heat removal from nuclear fuel, debris, underground disposal of radioactive waste material, storage of food stuffs, paper production, oil exploration etc (Kataria & Patel, 2019). The heat generated by the internal source can cause a temperature increase within the system and alter its thermal behavior. Internal heat sources play a crucial role in both natural and industrial processes. For example, in nuclear reactors, the heat generated by nuclear reactions is used to generate electricity. In combustion engines, the heat generated by fuel combustion drives the engine. In materials processing, such as welding and casting, heat generated by electrical resistance or chemical reactions is used to melt and. join materials. The heat generated by the internal source can create a temperature gradient, which can cause thermal stresses and material deformation. Therefore, understanding the behavior of internal heat sources is essential in designing and optimizing processes that involve heat generation, such as energy production and materials processing, to ensure the safety and effectiveness of the systems. Fluid flow problems with internal heat source has been investigated extensively (Vinod *et al.,* 2024). Ojemeri *et al.* (2024) presented an analytical investigation of a chemically reactive hydromagnetic fluid affected by heat generation/absorption flowing across a superhydrophobic microchannel that is heated alternatively. In addition, Ojemeri and Onwubuya (2023) described the analysis of steady mixed convection flow of Arrhenius-controlled chemical reaction and an exothermic fluid along an isothermally heated superhydrophobic microchannel due to heat source/sink.

In applied mathematics, perturbation theory comprises methods for finding an approximate solution to problem, by starting from the exact solution of a related simpler problem. A critical feature of the technique is a middle step that breaks the problem into ‘solvable’ and ‘perturbative’ parts. In perturbation theory, the solution is expressed as a power series in a small parameter. The first term is the known solution to solvable problem. Successive terms in the series at higher powers usually become smaller. An approximate ‘perturbation solution’ is obtained by truncating the series at higher powers, usually by keeping only the first two terms, the solution to the known problem and the ‘first order’ perturbation correction. Perturbation theory is used in a wide range of fields and reaches its most sophisticated and advanced forms in quantum field theory. Perturbation theory describes the use of this method in fluid mechanics. The field, in general remains actively and heavily researched across multiple disciplines (Kodi & Mopuri, 2022).

Recently, Patel (2025) studied motion with quadratic speed on the unsteady free convective MHD Casson fluid flow in a porous medium. The fluid in electrically conducting and bounding plate has ramped the surface concentration. The characteristics of heat and mass transfer are analyzed with thermal diffusion, heat generation, chemical reaction, and thermal radiation. Manthramurthy & Vempati (2025) researched on

the thermal and mass transfer properties of a magnetohydrodynamic Casson nanofluid flowing over a nonlinear porous stretching sheet subjected to a magnetic field. Their study considered chemical reactions, thermophoresis, non-uniform heat sources or sinks, and the Soret and Dufour effects. Furthermore, their analysis incorporated various slip parameters and a convective boundary condition.

The purpose of this paper was to analyze an important role of velocity slip effect on unsteady MHD flow of a Casson fluid flow past over a vertical plate in the presence of Soret parameter has been studied with heat source. This study is an extension of Anwar *et al.* (2021). The governing equations are solved by regular perturbation technique to obtain expressions for the velocity, temperature and concentration. Skin-friction, Nusselt and Sherwood numbers were also computed. The effects of important parameters on the velocity, temperature and concentration profiles were shown graphically and discussed.

2. Mathematical Formulation

Imagine the two-dimensional unsteady flow of an electrically conductive Casson fluid along an upright permeable plate affected by thermal radiation and suction impacts. The $x' - axis$ and $y' - axis$ are taken along the plate in the vertical upward and perpendicular direction to the plate respectively as illustrated in the schematic diagram (See Figure 1). It is assumed that a uniform strength B_0 is introduced transversely and normal to the plate, with no applied voltage signifying the absence of an electric field. Following Raju *et al.* (2016) and Anwar *et al.* (2021), and obeying the Boussinesq approximation, the governing equations of this current investigation can be expressed as follows:

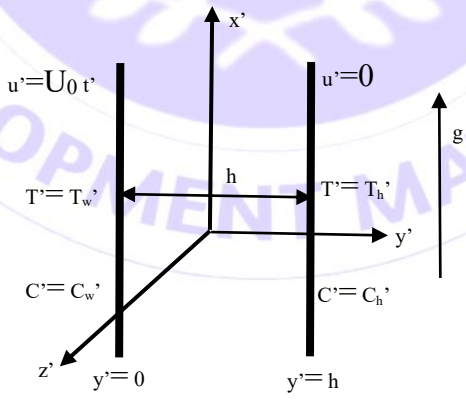

Figure 1: Schematic Diagram of the Flow System

Continuity Equation

$$\frac{\partial v}{\partial \xi} = 0 \tag{1}$$

Momentum Equation

$$\rho\left[\frac{\partial u}{\partial \tau} + v\frac{\partial u}{\partial \xi}\right] = \mu\left(1+\frac{1}{\beta}\right)\frac{\partial^2 u}{\partial \xi^2} - \delta\beta_0^2 u + \rho g\beta_T\left(T - T_\infty\right) + \rho g\beta_m\left(C - C_\infty\right) - \left(1+\frac{1}{\beta}\right)\frac{\mu\phi}{K_p}u \tag{2}$$

Energy Equation

$$\rho C_p\left[\frac{\partial T}{\partial \tau} + v\frac{\partial T}{\partial \xi}\right] = K\frac{\partial^2 T}{\partial \xi^2} - \frac{\partial Q_r}{\partial \xi} - Q_0\left(T - T_\infty\right) \tag{3}$$

Mass Equation

$$\frac{\partial C}{\partial \tau} + v\frac{\partial C}{\partial \xi} = D_m\frac{\partial^2 C}{\partial \xi^2} - K_1\left(C - C_\infty\right) + \frac{D_m K_T}{T_m}\frac{\partial^2 T}{\partial \xi^2} \tag{4}$$

The initial and boundary conditions are as follows:

$$\tau^* \le 0 : u^* = 0, \theta^* = T_\infty^*, \delta^* = C_\infty^* \text{ for all } \xi^*$$

$$\tau^* > 0 \begin{cases} u^* = \psi\dfrac{\partial u^*}{\partial y^*}, \theta^* = T_\infty^* + \left(T_w^* - T_\infty^*\right)\epsilon e^{iwt}, \delta^* = C_\infty^* + \left(C_w^* - C_\infty^*\right)\epsilon e^{iwt} \; at \; \xi^* = 0 \\ u^* \to 0, \theta^* \to T_\infty^*, \delta^* \to C_\infty^* \quad as \; \xi^* \to \infty \end{cases} \tag{5}$$

$$\frac{\partial v}{\partial \xi} = 0 \Rightarrow v = -v_c$$

The radiative heat flux term is simplified by making use of the Rosseland approximation as

$$q_r = -\frac{4\bar{\sigma}}{3k^*}\frac{\partial T^4}{\partial \xi} \tag{6}$$

Here, $\bar{\sigma}$ is Stefan – Boltzmann constant and k* is the mean absorption coefficient. It is assumed that the temperature differences within the flow are sufficiently small so that T^4 can be expressed as a linear function of T after using Taylor's series to expand T^4 about the free stream temperature T_∞ and neglecting higher – order terms. This results in the following approximation:

$$T^4 \cong 4T_\infty^3 T - 3T_\infty^4 \tag{7}$$

Using equations (6) and (7), in the second to the last term of equation (3), we obtain:

$$\frac{\partial q_r}{\partial \xi} = -\frac{16\bar{\sigma}T_\infty^3}{3k^*}\frac{\partial^2 T}{\partial \xi^2} \tag{8}$$

Introducing equation (8) into equation (3), we have:

$$\rho C_p\left[\frac{\partial T}{\partial \tau} + v\frac{\partial T}{\partial \xi}\right] = K\frac{\partial^2 T}{\partial \xi^2} + \frac{16\bar{\sigma}T_\infty^3}{3k^*\rho C_p}\frac{\partial^2 T}{\partial \xi^2} - Q_0\left(T - T_\infty\right) \tag{9}$$

We define the following dimensionless quantities:

$$\xi = \xi\frac{u_c}{\upsilon}, U^* = \frac{u^*}{u_c}, \tau^* = \frac{\tau u_c^2}{\upsilon}, \theta = \frac{T - T_\infty}{T_w - T_\infty}, \delta = \frac{C - C_\infty}{C_w - C_\infty} \tag{10}$$

Substituting equation (5) and using equation (1), equations (2), (4) and (9) become:

$$\frac{\partial U^*}{\partial \tau^*} - S\frac{\partial U^*}{\partial \xi^*} = \left(1 + \frac{1}{\beta}\right)\frac{\partial^2 U^*}{\partial \xi^{*2}} - \left(M + \left(1 + \frac{1}{\beta}\right)\frac{1}{K}\right)U^* + Gr\theta + Gm\delta \tag{11}$$

$$\frac{\partial \theta}{\partial \tau^*} - S\frac{\partial \theta}{\partial \xi^*} = \frac{1}{\Pr}\left(\frac{3R + 4}{3R}\right)\frac{\partial^2 \theta}{\partial \xi^{*2}} + \phi\theta \tag{12}$$

$$\frac{\partial \delta}{\partial \tau^*} - S\frac{\partial \delta}{\partial \xi^*} = \frac{1}{Sc}\frac{\partial^2 \delta}{\partial \xi^{*2}} - Kc\delta + Sr\frac{\partial^2 \theta}{\partial \xi^{*2}} \tag{13}$$

The corresponding initial and boundary conditions in non-dimensional form become:

$$U^* = U^* - \psi\left(\frac{\partial U^*}{\partial y}\right), \theta = 1 + \varepsilon e^{iwt}, \delta = 1 + \varepsilon e^{iwt}, at \quad \xi = 0$$

$$U^* \to 0, \theta \to 0, \delta \to 0 \quad \text{as} \quad \xi \to 0 \tag{14}$$

where, $Sc = \frac{\upsilon}{D_m}, M = \frac{\delta \beta_0^2 \upsilon}{\rho u_0^2}, Gr = \frac{\upsilon g \beta_T (T_w - T_\infty)}{u_0^3}, Gm = \frac{\upsilon \beta_m g (C_w - C_\infty)}{u_0^3}, Kc = \frac{K_1 \upsilon}{u_0^2},$

$S = \frac{v_c}{u_c}, R = \frac{Kk^*}{4\sigma T_\infty^3}, K = \frac{K_p u_c^2}{\upsilon^2}, Sr = \frac{D_m K_T}{T_m}\frac{(T_w - T_\infty)}{\upsilon (C_w - C_\infty)}, \phi = \frac{Q_0 \upsilon}{\rho C_p u_0^2}, \Pr = \frac{\mu C_p}{K}.$

3. Analytical Solutions

The equations (11) to (13) are coupled non-linear PDEs in dimensionless form. To solve these equations subject to the boundary conditions (14), dropping the (*), we assume solutions of the form:

$$U(\xi, \tau) = U_0(\xi) + U_1(\xi)\varepsilon e^{iwt} + o(\varepsilon) \tag{15}$$

$$T(\xi, \tau) = \theta_0(\xi) + \theta_1(\xi)\varepsilon e^{iwt} + o(\varepsilon) \tag{16}$$

$$C(\xi, \tau) = \delta_0(\xi) + \delta_1(\xi)\varepsilon e^{iwt} + o(\varepsilon) \tag{17}$$

where expressions for U_0, U_1, θ_0, θ_1, δ_0 δ_1 are to be determined. Furthermore, other higher terms of ε will be neglected i.e. only the first two terms are considered.

Substituting equation (15) to (17) into (11) to (14), gives:

$$U_0 : U_0'' + \frac{S}{\lambda}U_0' - \chi U_0 = -\frac{Gr}{\lambda}\theta_0 - \frac{Gm}{\lambda}\delta_0 \tag{18}$$

$$U_1 : U_1^{"} + \frac{S}{\lambda} U_1^{'} - \left(\frac{iw}{\lambda} + \chi \right) U_1 = -\frac{Gr}{\lambda} \theta_1 - \frac{Gm}{\lambda} \delta_1 \tag{19}$$

$$\theta_0 : \theta_0^{"} + \frac{\Pr S}{\gamma} \theta_0^{'} - \frac{\Pr \phi}{\gamma} \theta_0 = 0 \tag{20}$$

$$\theta_1 : \theta_1^{"} + \frac{\Pr S}{\gamma} \theta_1^{'} - \left(\frac{iw \Pr}{\gamma} + \frac{\Pr \phi}{\gamma} \right) \theta_1 = 0 \tag{21}$$

$$\delta_0 : \delta_0^{"} + ScS\delta_0^{'} - ScKc\delta_0 = -ScSr\theta_0^{"} \tag{22}$$

$$\delta_1 : \delta_1^{"} + ScS\delta_1^{'} - \left(iwSc + ScKc \right) \delta_1 = -ScSr\theta_1^{"} \tag{23}$$

The boundary conditions are:

$$U_0 - \psi \frac{du_0}{d\xi} = 0, \theta_0 = \theta_1 = 1, \delta_0 = \delta_1 = 1 \quad \text{at } \xi = 0 \tag{24}$$

$$U_0 = U_1 \to 0, \theta_0 = \theta_1 \to 0, \delta_0 = \delta_1 \to 0 \quad \text{as } \xi \to \infty$$

Solving equations (18) to (23) subject to boundary conditions (24), the solutions for the velocity, temperature and concentration are as follows, respectively:

$$U(\xi, \tau) = B_{12} e^{-f_{10}\xi} + B_{13} e^{-f_2 \xi} + B_{14} e^{-f_6 \xi} + B_{15} e^{-f_2 \xi} + (B_{17} e^{-f_{12}\xi} + B_{18} e^{-f_4 \xi} + B_{19} e^{-f_8 \xi} + B_{20} e^{-f_4 \xi}) \varepsilon e^{iwt} \tag{25}$$

$$\theta(\xi, \tau) = e^{-f_2 \xi} + (e^{-f_4 \xi}) \varepsilon e^{iwt} \tag{26}$$

$$\delta(\xi, \tau) = B_6 e^{-f_6 \xi} + B_7 e^{-f_2 \xi} + (B_9 e^{-f_8 \xi} + B_{10} e^{-f_4 \xi}) \varepsilon e^{iwt} \tag{27}$$

The Skin-friction, Nusselt and Sherwood numbers respectively are as follows:

$$C_f = -\left(\frac{dU^*}{d\xi} \right)_{\xi=0} = -f_{10} B_{12} - f_2 B_{13} - f_6 B_{14} - f2 B_{15} - (f_{12} B_{17} + f_4 B_{18} + f_8 B_{19} + f_4 B_{20}) \varepsilon e^{iwt}$$

(28)

$$Nu = -\left(\frac{d\theta}{d\xi}\right)_{\xi=0} = -f_2 - (f_4)\varepsilon e^{iwt} \tag{29}$$

$$Sh = -\left(\frac{d\delta}{d\xi}\right)_{\xi=0} = -f_6 B_6 - f_2 B_7 - (f_8 B_9 + f_4 B_{10})\varepsilon e^{iwt} \tag{30}$$

4. Result and Discussion

The velocity slip effect on unsteady magnetohydrodynamic (MHD) flow of Casson fluid in the presence of soret and heat source mechanisms has been formulated and solved analytically. The regular perturbation method was used to solve the governing equations of the flow field analytically. To have physical understanding of the problem, the velocity, temperature and concentration fields, numerical values have been assigned to the parameters of the flow.

4.1 Velocity profiles

Figure 1 displays the velocity profiles for different suction (S). The flux of the fluid in the boundary layer deceases when the intensity of the suction increases. Figure 2 shows velocity profiles for different values of Casson parameter (β). It is seen that larger value of Casson parameter lead to higher velocity profile which means there is larger thickness in the momentum boundary layer. In the case of varying values of Grashof number in mass transfer (G_m), the profiles of the velocity of the boundary layer is presented in Figure 3. As predicted, the fluid velocity is boosted and its maximum value is more pronounced when there is an increase in the buoyancy force $G_m$where by with a rise in G_m, there is also a rise in the velocity. Figure 4 presents the velocity profile for different values of Grashof number in the heat transfer (G_r). It is found that as G_r rises the velocity of the fluid increases. In the boundary layer, the velocity starts by increasing to a maximum, and slowly decreases. Physically, Grashof number indicates thermal buoyancy characteristic of a fluid flow. The greater it gets, the more the buoyant force brought about by the temperature gradient acts upon the fluid, thereby increasing its velocity rate in the vicinity of the heated surface. The peak velocity occurs in the boundary layer where the forces of buoyancy prevail over that of viscosity. Figure 5 depicts the velocity profiles for different values of magnetic field intensity (M). The flux of the fluid in the boundary layer decreases when the intensity of the magnetic field increases. The opposing direction of the fluid's flow is affected by the Lorentz force, which is the cause of this phenomenon. The fluid's velocity is accelerated,

leading to a perceptible dragging impact. The use of permeability parameter (K) in the velocity profile can be graphically represented as shown in Figure 6. The velocity boundary layer gets thicker as K increases. Physically, in the porous medium modeled as non-porous, i.e. ignoring the pore structure, the greater the K, the smaller the resistance in the medium. This will allow fluid to enter deeper which will subsequently increase the velocity boundary layer. Figure 7 illustrates the impact of Soret number (S_r)on the velocity profiles. It is observed that the velocity increases as S_r becomes significant. The impact of chemical reaction parameter (K_c) on the velocity profile is presented in Figure 8. It is evident that the momentum boundary layer becomes lower as (K_C) is increased. The velocity profiles of Figure 9 demonstrate the velocity profiles at some Schmidt number (S_C). The velocity decreases with increase in S_C. Figure 10 displays the velocity profiles for different values of (P_r). It is notice that the velocity decreases as P_r rises. In Figure 11, the impact of heat absorption parameter on the velocity profiles is shown. It is clear that the velocity boundary layer decreases when the heat absorption is increased. Figure 12 connotes the velocity profile for varied values of radiation parameter (R). It is seen that higher value of R lead to rise in the velocity of the fluid. Figure 13 shows the effect of velocity slip on the velocity of the fluid. It is evident that higher values of the velocity slip parameter cause a rise in the fluid velocity.

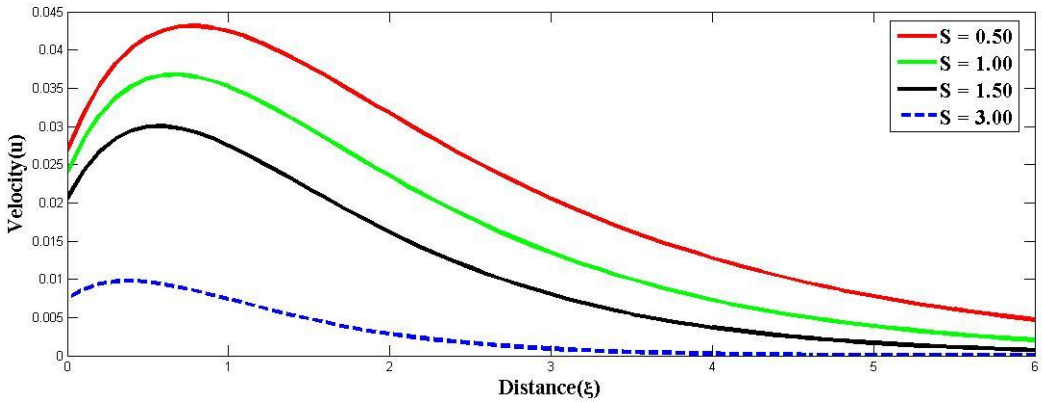

Figure 1: Velocity profile for different values of S.

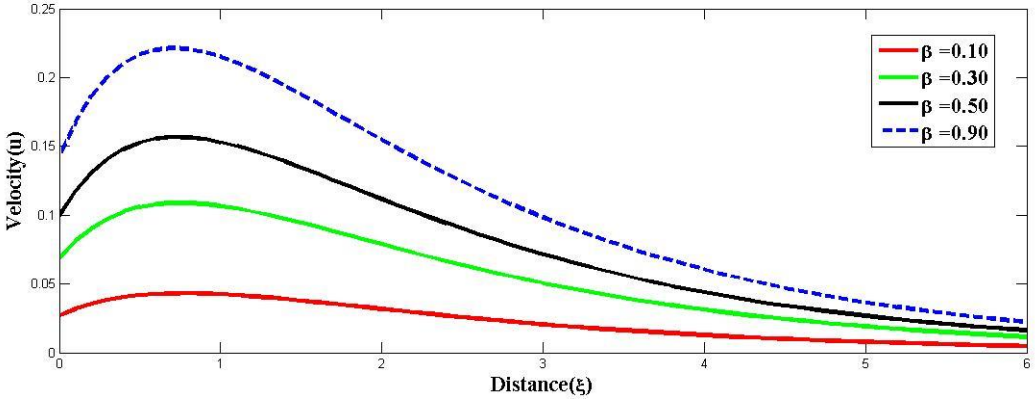

Figure 2: Velocity profile for different values of β.

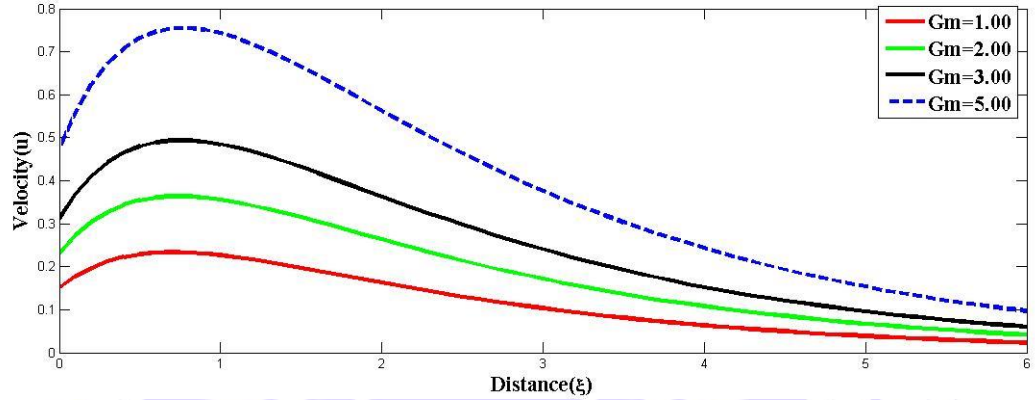

Figure 3: Velocity profile for different values of Gm.

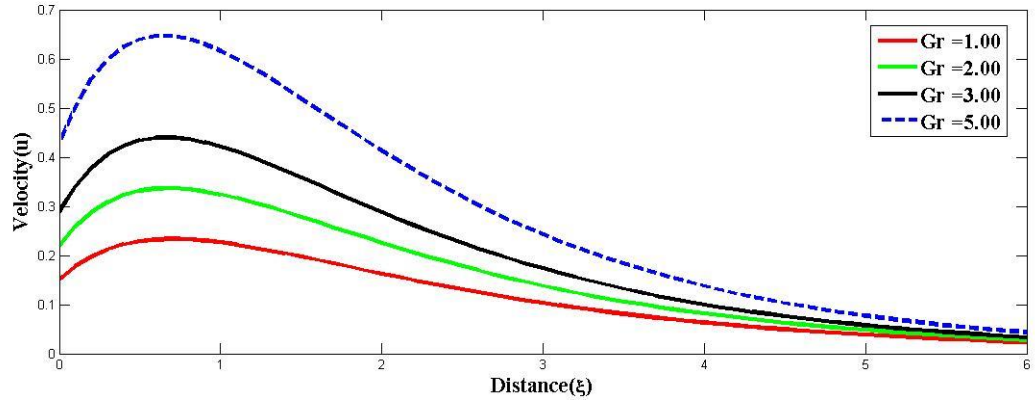

Figure 4: Velocity profile for different values of Gr.

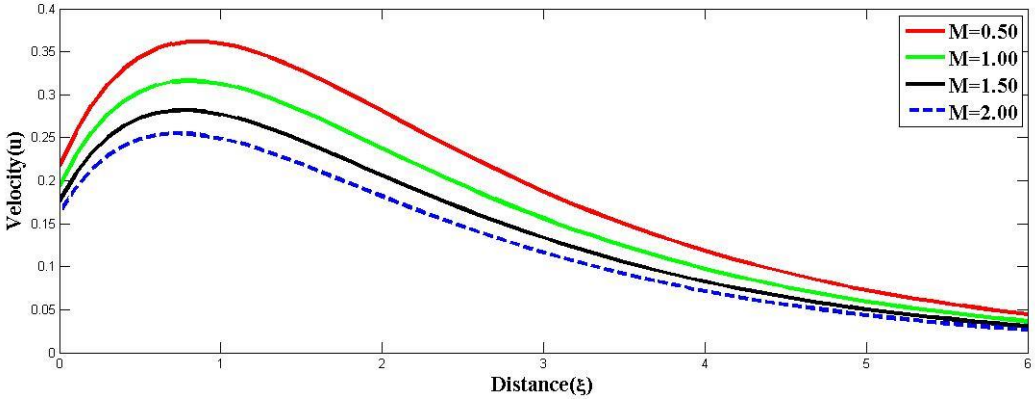

Figure 5: Velocity profile for different values of M.

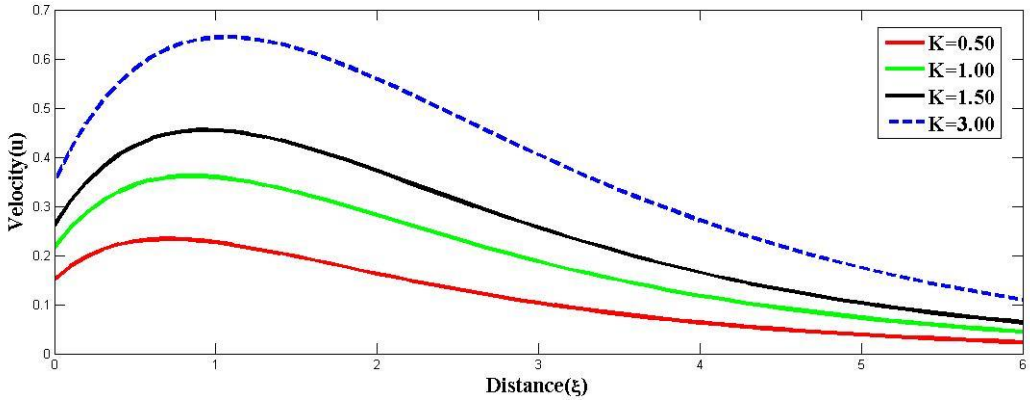

Figure 6: Velocity profile for different values of K.

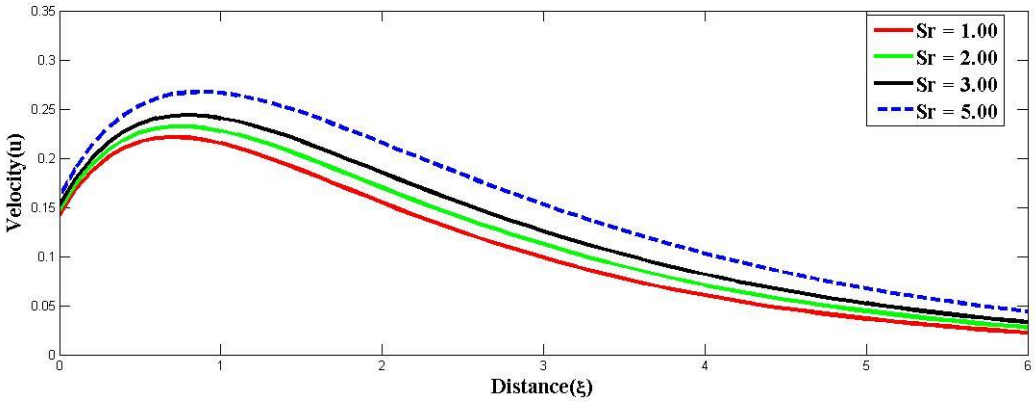

Figure 7: Velocity profile for different values of Sr.

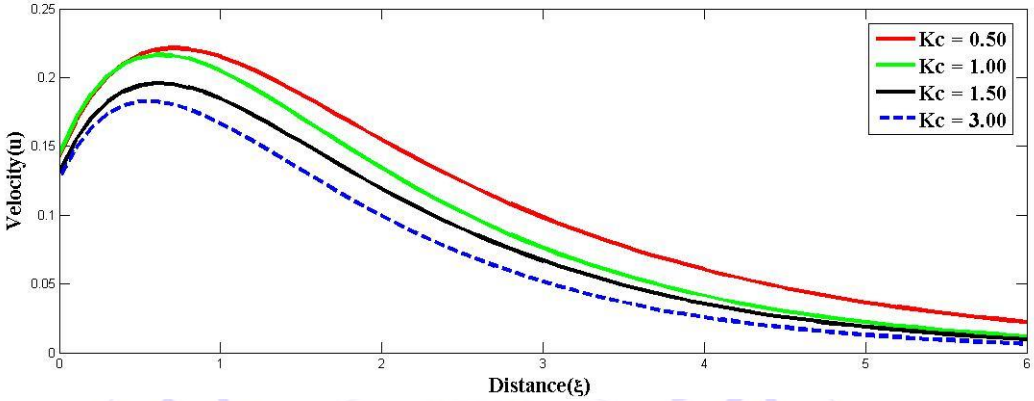

Figure 8: Velocity profile for different values of Kc.

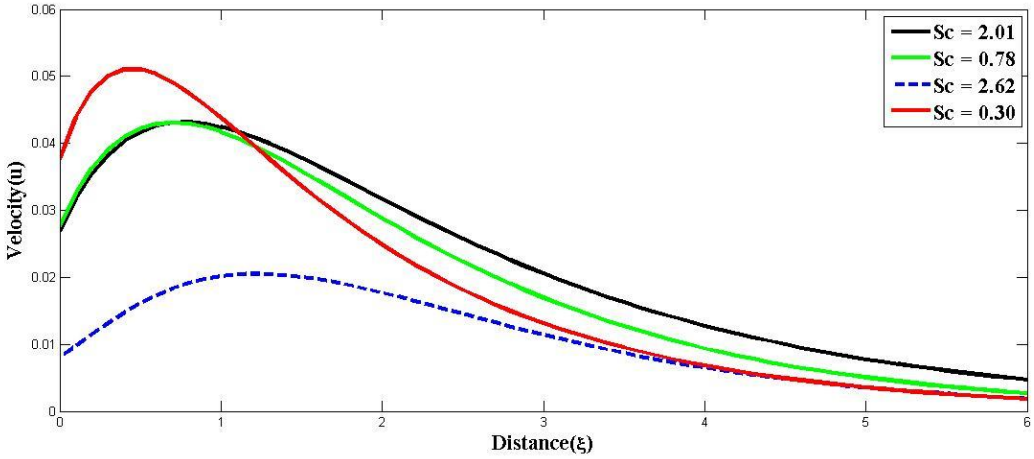

Figure 9: Velocity profile for different values of Sc.

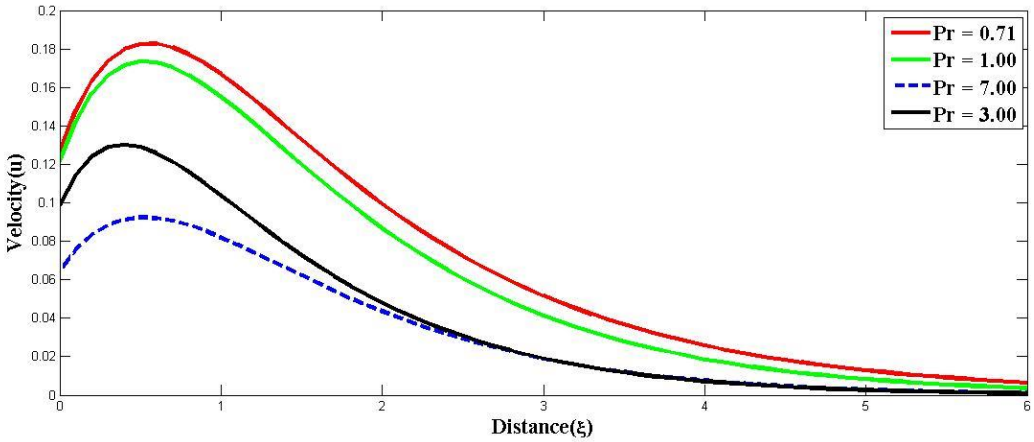

Figure 10: Velocity profile for different values of Pr.

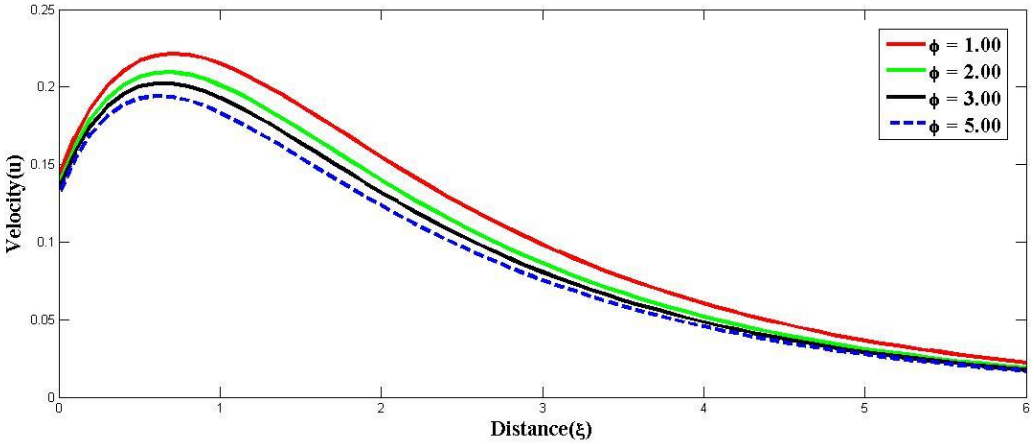

Figure 11: Velocity profile for different values of ϕ.

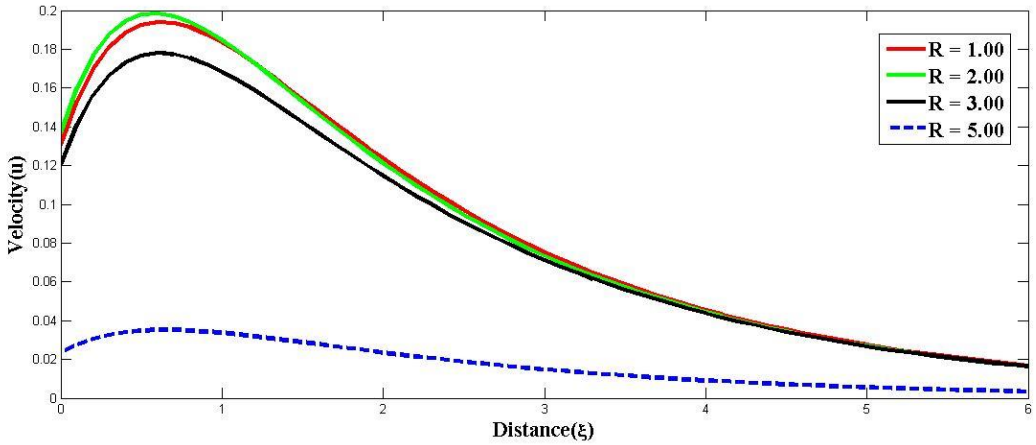

Figure 12: Velocity profile for different values of R.

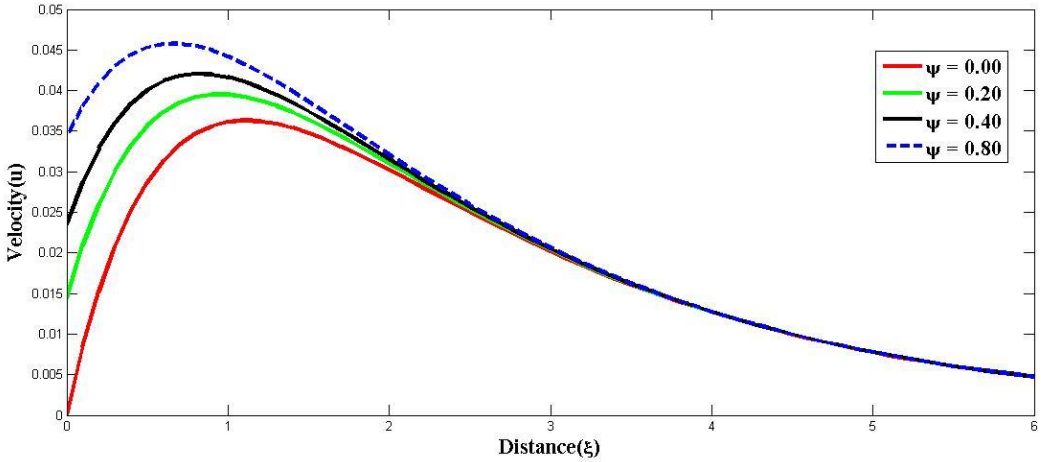

Figure 13: Velocity profile for different values of ψ.

4.2 Temperature profile

Figure 14 represents the impact of S on the temperature profiles. It is found that increase in suction causes an increase in the thermal boundary layer of the fluid. The influence of the Prandtl number on the temperature field is displayed in Figure 15. Because the heating capacity of the fluid reduces with increase in Pr, causing the boundary of the thermally layer to be thinner. It is obvious that increase in Prandtl value will decrease the temperature of the fluid. Figure 16 displays velocity profiles for different values of ϕ. It is seen that the momentum boundary layer decreases as ϕ become significant. Figure 17 discovers the effect

of radiation factor on the temperature. It shows that responsive manipulation of the radiation parameter R (which represent intensity of heating energy or radiative heat input) produces different effects on the fluid temperature distribution. With increase in R, i.e. when more radiative heat is introduced, the area around the boundary region gets far warmer. This is the case since the radiation directly introduces thermal energy into the fluid, increasing its temperature within the boundary layer.

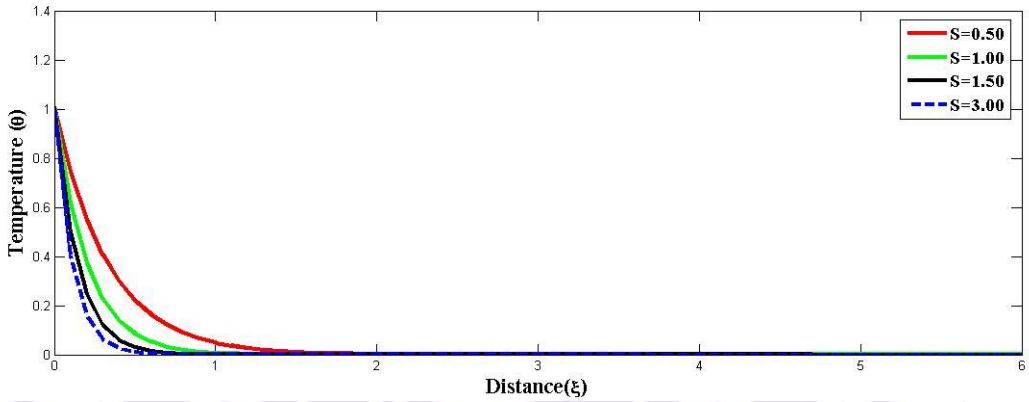

Figure 14: Temperature profile for different values of S.

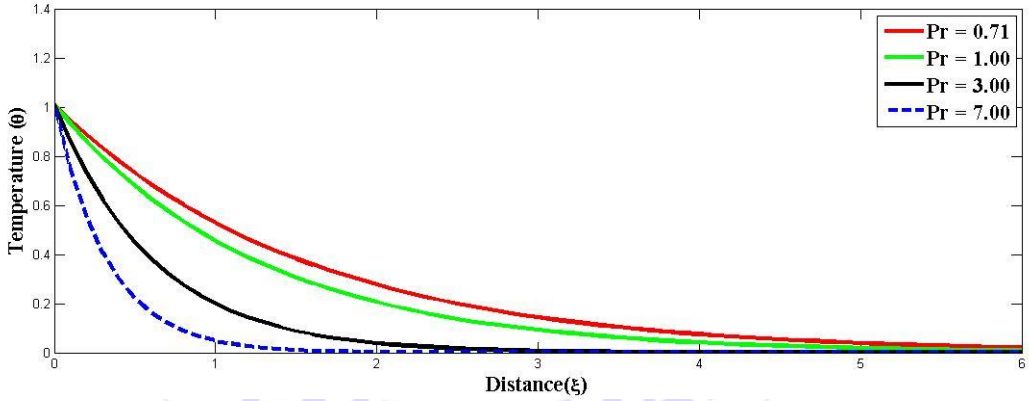

Figure 15: Temperature profile for different values of Pr.

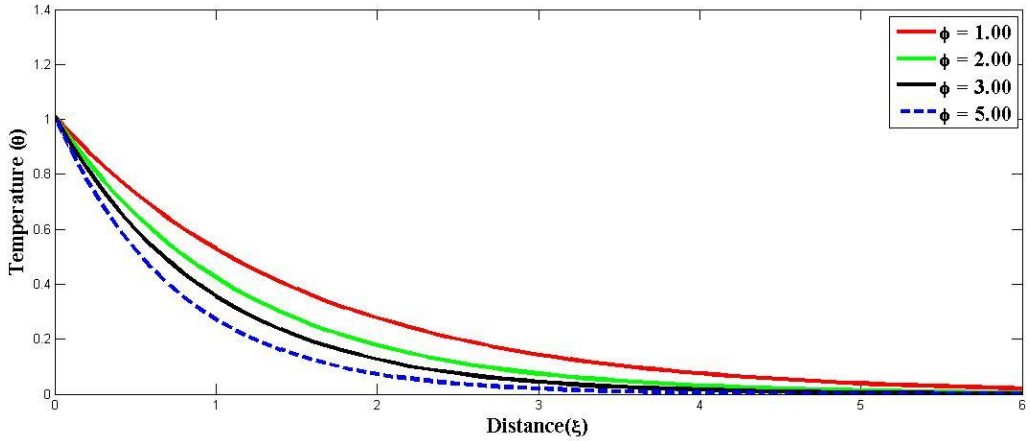

Figure 16: Temperature profile for different values of ϕ.

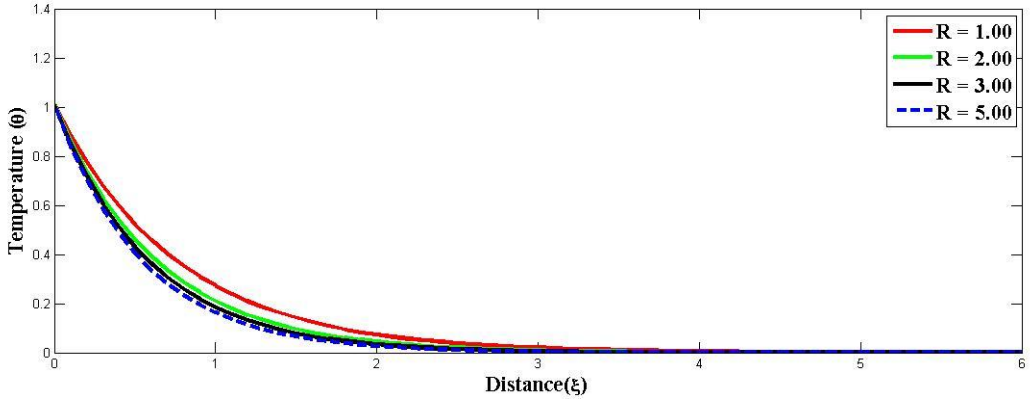

Figure 17: Temperature profile for different values of R.

4.3 Concentration profile

Figure 18 depicts the effect of suction on the concentration profiles. It is seen that the concentration of the fluid becomes lower as suction becomes significant. The concentration profiles of Figure 19 demonstrate the concentration profiles at some Schmidt values. The concentration decreases with increase in Schmidt value (Sc). The causes a narrower concentration boundary layer and reduced penetration of a solute in the fluid. Because the steeper concentration gradients are associated with slower diffusion of mass with increasing Sc. This causes a narrower concentration boundary layer and reduced penetration of a solute in the fluid. Figure 20 shows the plot of the concentration profiles for different values of Soret number. It is seen that the mass boundary layer decreases as Sr is increased. Soret effect or thermal diffusion refers to

mass flow developed because of differences in temperature. The Soret effect accelerates the mass transfer between the fluid through the fluid space, hence, making the fluid to have a lowered concentration. The effect of chemical reaction on the concentration of the fluid is depicted in Figure 21. It is clear that the fluid's concentration rises and the chemical reaction parameter is increased.

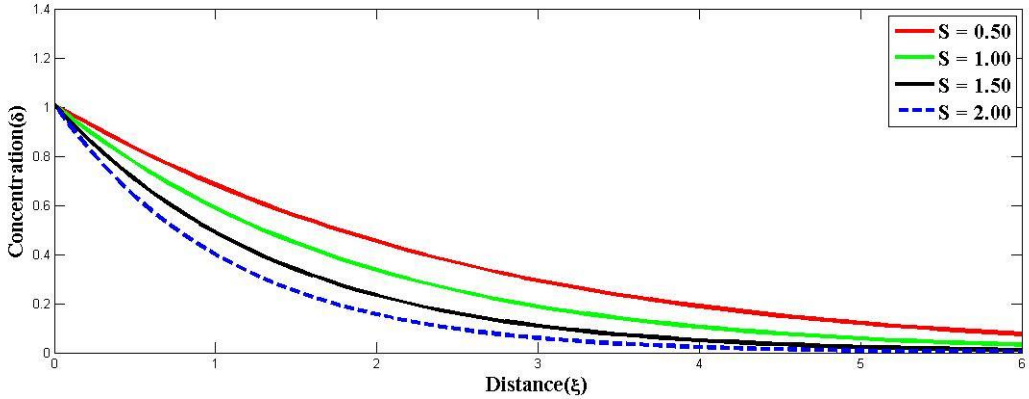

Figure 18: Concentration profile for different values of S.

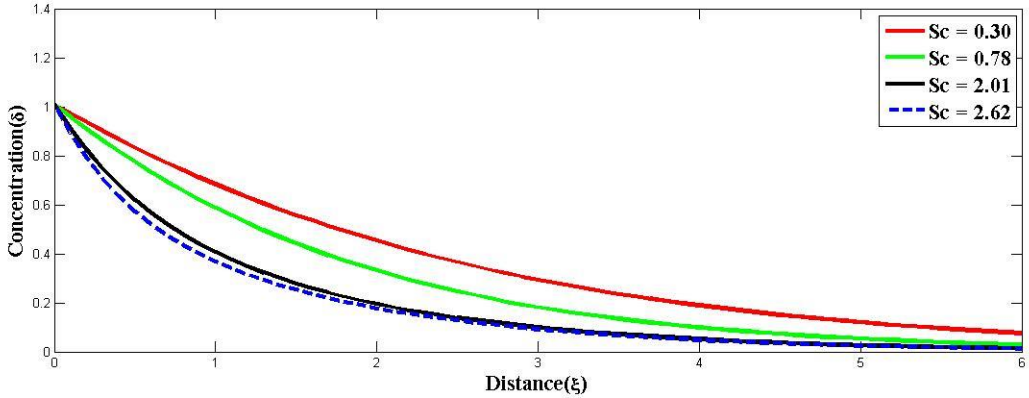

Figure 19: Concentration profile for different values of Sc.

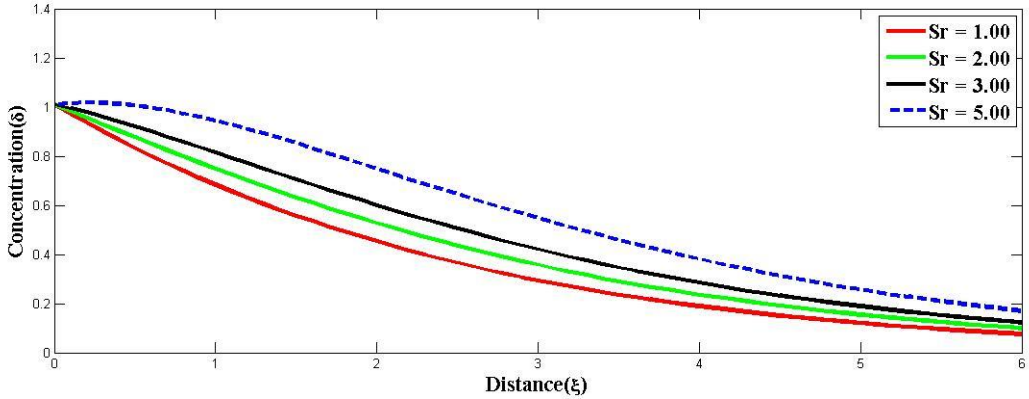

Figure 20: Concentration profile for different values of Sr.

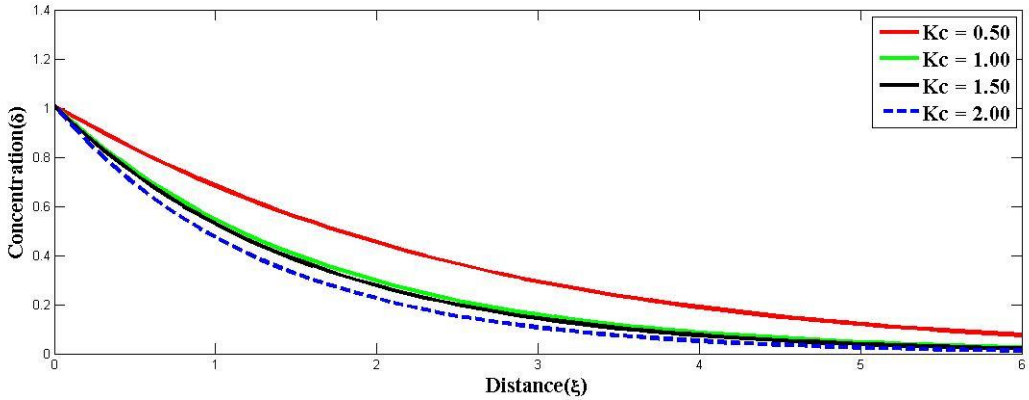

Figure 21: Concentration profile for different values of Kc.

5. Conclusion

The current paper gives the analytical solution of velocity slip effect on unsteady Magnetohydrodynamic (MHD) flow of Casson fluid in the presence of Soret and heat source mechanisms. Specifically, the governing boundary layer equations are made up with suitable boundary conditions. The boundary layer equations are simplified and non-dimensionalized. The velocity, temperature and concentration have also been expressed which was achieved by regular perturbation method. The influence of the relevant parameters on the velocity, temperature and concentration profiles are illustrated graphically. The most significant conclusion are as follows:

1. Setting the parameters, Soret, velocity slip and radiation equal to zero the results of Kateria and Petal (2019) is gotten. Also, neglecting mass transfer and Soret effect in the present study agrees with the research conducted by Anwar *et al.* (2021).

2. The velocity declines with the effect of the strength of magnetic field, suction, chemical reaction, heat source and radiation and it grows in an increase in permeability parameter, Casson parameter, Soret number, velocity slip parameter, mass and thermal Grashof numbers.

3. The temperature and the thickness of thermal boundary layer decrease with an increase in the radiation, Prandtl number, heat source and suction.

4. The concentration reduces the Schmidt number, chemical reaction and suction increases but increases as Soret number becomes significant.

References

Ahmad, S., Ul Haq, S., Ali, F., Khan, I. and Sayed M. Eldin, S.M. (2023). Free convection channel flow of couple stress Casson fluid: A fractional model using Fourier's and Fick's laws. *Frontiers in Physics*. 1-3. doi: 10.3389/fphy.2023.1031042.

Ahmad, A. & Sarki, M. N. (2023). Slip condition effects on unsteady MHD fluid flow with radiative heat flux over a porous medium. *Advances in Pure Mathematics*, 13, 153-166. https://doi.org/10.4236/apm.2023.13300

Akolade, M. T., Idowu, A. S., & Adeosun, A. T. (2021). Multislip and Soret–Dufour influence on nonlinear convection flow of MHD dissipative casson fluid over a slendering stretching sheet with generalized heat flux phenomenon. *Heat transfer*, *50*(4), 3913-3933. **https://doi.org/10.1002/htj.22057**

Anwar, T., Kumam, P. & Watthayu, W. (2021). Unsteady MHD natural convection flow of Casson fluid incorporating thermal radiative flux and heat injection/suction mechanism under variable wall conditions. *Journal of scientific reports.* 11,4275. https://doi.org/10.1038/s41598-021-83691-2.

Babu, R.S., Venkateswarlu, S., Lakshmic, J.K. (2018). Effect of magnetic field and radiation on MHD heat and mass transfer of micropolar fluid over stretching sheet with Soret and Dufour effects. *International Journal of Applied Engineering Research.* 13(12), 10991–11000. ISSN 0973-4562. http://www.ripublication.com

Casson, N. (1959). A flow equation for pigment-oil suspensions of the printing ink type. Rheology of Disperse Systems.

Chaudhary, H., Singh, N., Roshan, M., Yadav, P. K., & Saleem, S. (2025). Modeling of magnetohydrodynamic Casson fluid flow due to moving permeable plate with Soret and Dufour impacts. *Journal of the Korean Physical Society*, 1-24. https://doi.org/10.1007/s40042-025-01301-0

Goud, B. S. & Reddy, Y. D. (2022). Chemical reaction and Soret effect on an unsteady MHD heat and mass transfer fluid flow along an infinite vertical plate with radiation and heat absorption. Journal of the

Indian Chemical Society, 99. https://doi.org/10.1016/j.jics.2022.100762.

Goud, B. S., Reddy, Y. D., & Asogwa, K. K. (2023). Chemical reaction, Soret and Dufour impacts on magnetohydrodynamic heat transfer Casson fluid over an exponentially permeable stretching surface with slip effects. *International Journal of Modern Physics B*, *37*(13), https://doi.org/10.1142/S0217979223501242.

Jangida, S. and Kolla, K. (2025). Magnetic field and Soret effect on mixed convection Williamson fluid flow between two concentric cylinders using artificial neural network. *European Physical Journal Plus.* 140:220 https://doi.org/10.1140/epjp/s13360-025-06175-6.

Kataria, H. R. and Patel, H. R. (2019). Effects of chemical reaction and heat generation/absorption on magnetohydrodynamic (MHD) Casson fluid flow over an exponentially accelerated vertical plate embedded in porous medium with ramped wall temperature and ramped surface concentration. *Propulsion and power research.* 8(1):35-46. https//doi.org/10.1016/j.jppr.2018.12.001.

Kodi, R., & Mopuri, O. (2022). Unsteady MHD oscillatory Casson fluid flow past an inclined vertical porous plate in the presence of chemical reaction with heat absorption and Soret effects. *Heat Transfer*, *51*(1), 733-752.**https://doi.org/10.1002/htj.22327**

Krishna, M. V., & Reddy, B. P. (2025). Thermal radiation, heat source, and chemical reaction impacts on MHD convective flow of casson fluid past an infinite inclined oscillating vertical porous plate. *Multiscale and Multidisciplinary Modeling, Experiments and Design*, *8*(3), 196. https://doi.org/10.1007/s41939-025-00774-7

Manthramurthy, P., & Vempati, S. R. (2025). Significance of multiple slips and thermal radiation on heat and mass transfer in MHD Casson nanofluid flow over an exponentially stretching porous sheet with non-uniform heat source and sink. *Multiscale and Multidisciplinary Modeling, Experiments and Design*, *8*(3), 1-18. https://doi.org/10.1007/s41939-025-00743-0

Ojemeri, G. and Onwubuya, I. O. (2023). Analysis of mixed convection flow on arrhenius-controlled heat generating/absorbing fluid in a superhydrophobic microchannel: A semi-Analytical Approach, Dutse. *Journal of Pure and Applied Sciences.* 9, 344-357. https://doi.org/104314/dujopas.v9i2a.34.

Ojemeri, G., Onwubuya I. O., Omokhuale, E., Hussaini A. and Shuaibu, A. (2024). Analytical investigation of arrhenius kinetics with heat source/sink impacts along a heated superhydrophobic microchannel. *UMYU Scientifica,* 3(1), 61-71. DOI: https://doi.org/105619/usci.2431.004.

Patel, H. R. (2025). Soret and heat generation effects on unsteady MHD Casson fluid flow in porous medium. *Waves in Random and Complex Media*, *35*(1), 1172-1195. https://doi.org/10.1080/17455030.2022.2030500

Rajakumar, K. V.B., Pavan Kumar, V. S. R., Balamurugan, K. S. and Bharat, V. K. (2020). Unsteady MHD Casson dissipative fluid flow past a semi-infinite vertical porous plate with radiation absorption and chemical reaction in presence of heat generation. *Journal of Mathematical Modelling of Engineering Problems.* 7(1), 160172. https://doi.org/10.18280/mmep.070120.

Raju, R. S., Reddy, G. J., Raoc, J. A. and Rashidi, M. M. (2016). Thermal diffusion and diffusion thermo effects on an unsteady heat and mass transfer magnetohydrodynamic natural convection couette flow using FEM. *Journal of Computational Design and Engineering*. 3, 349–362. https://dx.doi.org/10.1016/j.jcde.2016.06.003.

Srinivas, S., Kumar, C. K., & Reddy, A. S. (2022). Dufour and Soret effects on pulsatile hydromagnetic flow of Casson fluid in a vertical non-Darcian porous space. *Nonlinear Analysis: Modelling and Control*, *27*(4), 669-683. https://doi.org/10.15388/namc.2022.27.26678

Usman, H., Uwanta I. J. and Sanusi, Z. (2022). Thermal diffusion and diffusion- thermo effects on ohmic heating with MHD free convective flow past a vertical porous plate in the presence of viscous dissipation. *Nigerian Journal of mathematics and Applications.* 32(1), 259-285.

Uwanta, I. J. and Hamza, M. M. (2014). Unsteady flow of reactive viscous, heat generating/absorbing fluid with soret and variable thermal conductivity. *International Journal of Chemical Engineering*. https://doi.org/10.1155/2014/291857.

Ullah, I., Khan, I., & Shafie, S. (2017). Soret and Dufour effects on unsteady mixed convection slip flow of Casson fluid over a nonlinearly stretching sheet with convective boundary condition. *Scientific Reports*, *7*(1), 1113. https://doi.org/10.1038/s41598-017-01205-5

Vinod, Y., Suma N. N., Raghunatha, K. R. and Sangamesh (2024). Dufour and Soret effects on double diffusive Casson fluid flow with the influence of internal heat source. *Journal of Umm Al-Qura University for Applied Sciences*. Pp 1-5. https://doi.org/10.1007/s43994-024-00133-1.